Thermal spin transition of circularly shaped nanoparticles in a core-shell structure investigated with an electroelastic model

A. Slimani,[1,*] K. Boukheddaden,[2,†] and K. Yamashita[1]

[1]*Department of Chemical System Engineering, The University of Tokyo, 7-3-1, Hongo, Bunkyo-Ku, Tokyo 113-8656, Japan*
[2]*Groupe d'Etudes de la Matière Condensée, CNRS–Université de Versailles, 45 Avenue des Etats Unis, F-78035 Versailles Cedex, France*

The functionalization of spin crossover materials as nanoscopic devices is a big challenge to overcome. It will entail a detailed exploration of why and how size reduction affects spin crossover behavior. We investigated the thermal spin transition of a nanoparticle in a core-shell structure as a function of particle size, the intensity of interactions between molecules, and also the thickness of the shell and its stiffness. The analysis was performed using an electroelastic model based on Monte Carlo methods on a distortable two-dimensional lattice, the sites of which are occupied by high-spin or low-spin atoms. Such analysis reflects the crucial influence of size as well as of the surrounding environment on the behavior of the spin transition, and it provides reliable explanations based on the elastic properties of the system.

I. INTRODUCTION

Switchable molecular solids such as spin transition compounds [1] still stimulate a particular interest among scientists due to their bistable states, which are accessible using different external stimuli such as temperature, light, pressure, magnetic field, and more recently electric field [2–10]. Such molecular flexibility indicates a considerable capability and promising prospects in highly technological applications. To be integrated in functional devices, spin crossover compounds should maintain their bistability at the nanometer scale. Recently, several extensive research efforts have been devoted to the study of the thermodynamic properties of spin crossover compounds [9,11–21]. However, extrapolation from bulky behaviors to nanosized systems is a serious challenge for scientists. In fact, the decreasing size of the materials adds further barriers to overcome, such as the confinement as well as interface effects. Although there has been chemical success in reproducing a spin transition at the nanometer scale, many obstacles remain. These include a marginal change in the transition temperature and the partial character of the transition. Several experimental investigations have focused on the environment effect [22] as well as the size effect on the thermal spin transition [9,11–21], however very few theoretical attempts have been devoted to exploring the physical mechanisms governing the bistability of spin crossover nanoparticles and their potential behavior changes through their interaction with their immediate environment. In this context, the Ising-like model [23] with forced high-spin (HS) molecules at the surface (accounting for the weakness of the ligand field at the surface) and elastic models [24] were introduced to explain the experimental observations of individual spin crossover (SC) nanoparticles and those embedded in a matrix, respectively. Despite the success of these studies, many aspects are still unclear and need further investigations. In particular, the role of the lattice symmetry and the shape of the nanoparticles on

their cooperative character merits closer examination with a view to identifying new properties.

In this paper, we investigate the thermal spin transition of a circularly shaped SC nanoparticle with forced HS molecules at the edge by means of an electroelastic model. To be general, we considered a nanoparticle in a core-shell structure. The core-shell system here refers to the inner core with spin crossover properties, while the outer shell consists of inactive materials not involved in the spin transition. From an experimental point of view, usually the shell acts as a protective layer to strengthen the core performances or to bring new properties such as fluorescence, which leads to bifunctional spin crossover/luminescence nanoparticles [25]. The previously used electroelastic model has demonstrated an ability to investigate the interplay between elastic interactions in a core-shell model for square-shaped spin-crossover nanoparticles [26]. The added value of this work regarding the contribution cited previously entails (i) investigating the thermal spin crossover transition with regard to the different structural parameters of the particle, and (ii) providing insight into the effect of the shape on the different laws that govern thermal behavior. Here, we focus on a systematic investigation of the different structural parameters of a spin crossover nanoparticle, while in our previous work [26] we focused mainly on the size effect of the system. The paper is organized as follows: In Sec. II, we present the electroelastic Hamiltonian and we describe the simulation procedure. In Sec. III, we study the behavior of the thermal spin transition of the circular nanoparticles as a function of their size, the interaction, the shell's stiffness, and the shell's thickness. In Sec. IV, we conclude.

II. THE MODEL: CALCULATION DETAILS

We consider a two-dimensional (2D) circularly shaped lattice with fixed topology and open boundary conditions. The core-shell structure is described by an inner spin crossover core, where the spins and positions of each node can be changed through the usual Monte Carlo procedure. The outer

---

*ahmed@tcl.t.u-tokyo.ac.jp
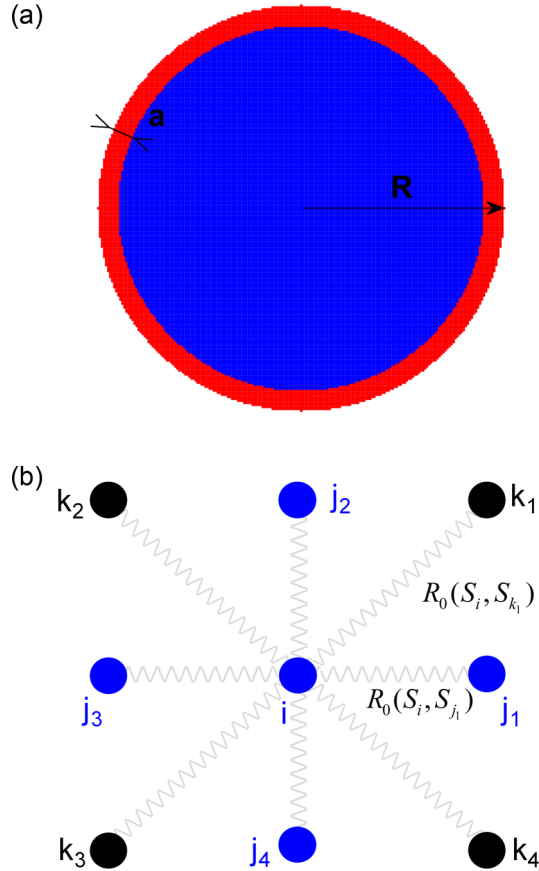†kbo@physique.uvsq.fr

(a)

(b)

FIG. 1. (Color online) (a) Schematic representation of the studied core-shell system, r is the radius of the nanoparticle and a represents the thickness of the shell consisted by atoms forced in the HS state. (b) Topology of bonds between the node i and its nearest (next-nearest) neighbors j_α (k_α). At equilibrium, the interaction length between the nearest (next-nearest) neighbors is $R_0(S_i,S_j)$ [$R_0(S_i,S_k)$].

layer acts as a shell represented by nodes locked in the HS state, and only their positions are changed by the Monte Carlo procedure. The atoms can move only inside the plane. To justify the choice of the HS shell, we assume that, in the case of nanoparticles, molecules located on the surface (here the border) experience a weaker ligand field, which forces them to stay in the HS state. A schematic representation of the studied nanoparticle system is reported in Fig. 1(a). The nodes of the system are placed to establish a square symmetry, where each node has four nearest neighbors (NNs) and four next-nearest neighbors (NNNs), as shown in Fig. 1(b). The nodes of the lattice are considered as spin crossover molecules and may have two spin states, high-spin (HS) and low-spin (LS), described by the respective eigenvalues $+1$ and -1 of an associated fictitious spin S. The distance and the interactions between the molecules depend on their spin states. In fact, the interactions between NN and NNN can be considered through springs whose stiffness depends on the instantaneous distance between the sites. The total Hamilto-

nian of the system, taking into account electronic and elastic contributions, reads

$$H = \sum_i \frac{(\Delta - k_B T \ln g) S_i}{2} + \sum_{i,j} A_{ij}[r_{ij} - R_0(S_i,S_j)]^2$$
$$+ \sum_{i,k} B_{ik}[r_{ik} - R_0'(S_i,S_k)]^2. \tag{1}$$

This Hamiltonian was introduced earlier in a previous work [27]. We recall that the first term of Hamiltonian (1) contains the ligand-field energy, Δ, and the entropic contribution, $-k_B T \ln g$, arising from the degeneracy g (electronic, orbital, and vibrational) of the spin states. The second and third terms account for the elastic interactions between NN and NNN spin crossover units, respectively. $R_0(S_i,S_j)$ is the equilibrium bond lengths between two nodes i and j depending on the bond type; $R_0(+1,+1) = R_0^{HH}$, $R_0(+1,-1) = R_0(-1,+1) = R_0^{HL}$, and $R_0(-1,-1) = R_0^{LL}$, where R_0^{HH}, R_0^{HL}, and R_0^{LL} are the respective equilibrium distances between HS-HS, HS-LS, and LS-LS sites. It is straightforward to demonstrate that

$$R_0(S_i,S_j) = \rho_0 + \rho_1(S_i + S_j) + \rho_2 S_i S_j, \tag{2}$$

where $\rho_0 = \frac{(R_0^{HH} + 2R_0^{HL} + R_0^{LL})}{4}$, $\rho_1 = \frac{(R_0^{HH} - R_0^{LL})}{4}$, and $\rho_2 = \frac{(R_0^{HH} - 2R_0^{HL} + R_0^{LL})}{4}$.

In the Hamiltonian (1), $A_{ij}(S_i,S_j)$ [$B_{ik}(S_i,S_k)$] denotes the local bond stiffness of NN (NNN) bonds and is written under the following form so as to decrease the total elastic constant in the HS spin state: $A_{ij}(r_{ij}) = A_0 + A_1(r_{ij} - R_0^{HH})^2$ and $B_{ik}(r_{ik}) = B_0 + B_1(r_{ik} - \sqrt{2}R_0^{HH})^2$. A_0 (B_0) and A_1 (B_1) are, respectively, the harmonic and the anharmonic contributions to the elastic interaction energy between NN (NNN) neighbors, while $r_{ij} = \|\vec{r}_i - \vec{r}_j\|$ (r_{ik}) is the instantaneous distance between two NN (NNN) sites.

The Monte Carlo procedure was executed on both spin and position variables. The stochastic algorithm is performed in the following way: for a site i randomly selected, with spin ($S_i = \pm 1$) and position $\vec{r}_i$, a new spin value S_i ($= -S_i$) will be set without position change. This spin change is accepted or rejected by the usual METROPOLIS criterion. Once the new spin value is accepted, the lattice is relaxed mechanically by a slight motion of each node selected randomly with a quantity $\|\delta\vec{r}_i\| \ll \|\vec{r}_i\|$. Afterward, a new site will be selected randomly, and so on. Once all the nodes of the lattice are visited for the spin change, we define such a step as the Monte Carlo step (MCS) unit. The adopted kinetic temperature is defined as the system is first cooled down from 400 to 0 K and then warmed up until 400 K. In both ways, the thermal increment is 1 K. For each temperature, 10^3 MCSs were required. In the present model, we use (as much as is possible) realistic parameter values derived from experimental data. Thus, we take for ligand-field energy $\Delta = 1500$ K and for the degeneracy ratio $g = 150$ [28–30] leading to an entropy change at the transition $\Delta S = N k_B \ln g = 82 \text{ J K}^{-1} \text{Mol}^{-1}$ and a transition temperature $T_{eq} = \frac{\Delta}{k_B \ln g} \approx 300$ K.

The equilibrium distances in the LS and HS states are, respectively, $R_0(-1,-1) \approx 1$ nm and $R_0(+1,+1) \approx 1.2$ nm, while for the HL state we consider $R_0(+1,-1) \approx \frac{[R_0(+1,+1)+R_0(-1,-1)]}{2} = 1.1$ nm. The lattice parameter between

NNN HS (LS) atoms is simply given by $\sqrt{2}R_0(+1,+1) \approx 1.7$ nm [$\sqrt{2}R_0(-1,-1) \approx 1.4$ nm].

III. RESULTS AND DISCUSSION

The Hamiltonian as written in Eq. (1) does not express clearly the connection between the electronic (spin states) and the elastic (atomic positions) degrees of freedom of the core-shell particles. Therefore, we reexpress Eq. (1) in terms of an Ising-like Hamiltonian with space-dependent effective interaction and field [27]. After simple developments, we get the expression of Hamiltonian (3), where for simplicity we show only the harmonic contributions and the elastic interactions between the first nearest neighbors,

$$H = \sum_{i-j} J_{ij} S_i S_j + \sum_i h_i S_i + \frac{A_0}{2} \sum_{i-j} (r_{ij} - \rho_0)^2 + C. \quad (3)$$

There, the parameters J_{ij} and h_i are the local exchangelike interactions and the local fieldlike contributions, respectively. The expressions of J_{ij} and h_i are given by

$$J_{ij} = A_0\big[\rho_1^2 - \rho_2(r_{ij} - \rho_0)\big] \quad (4)$$

and

$$h_i = \frac{1}{2}(\Delta - k_B T \ln g) + \frac{z}{2} A_0 \rho_1 \rho_2 - A_0 \rho_1 \sum_{j=1}^{z}(r_{ij} - \rho_0), \quad (5)$$

where the index j runs over the neighbors of a given site i, and z (=4) is the coordination number. The constant C is given by

$$C = \frac{zN}{4} A_0 \big(2\rho_1^2 + \rho_2^2\big), \quad (6)$$

and it will be omitted hereafter, since it does not play any role in the thermodynamic properties of the system. The third term of Eq. (3) is related to the cohesion energy of the lattice, whose equilibrium distance is given by ρ_0. It is interesting to mention that the general structure of the interaction parameter J_{ij} shows that the present model allows to generate both short- and long-range interactions, via the respective two-site contributions, $A_0 \rho_1^2 S_i S_j$ and $-A_0 \rho_2 (r_{ij} - \rho_0) S_i S_j$. In addition, the fieldlike structure shows also an electronic and elastic contribution, easily identified in Eq. (5).

In the present simulations, we have used $R_0^{HL} = \frac{(R_0^{HH} + R_0^{LL})}{2}$, and therefore $\rho_2 = 0$, which leads to the following expressions of J_{ij} and h_i:

$$J_{ij} = A_0 \rho_1^2 \quad (7)$$

and

$$h_i = \frac{1}{2}(\Delta - k_B T \ln g) - A_0 \rho_1 \sum_{j=1}^{z}(r_{ij} - \rho_0). \quad (8)$$

To express the equilibrium temperature as a function of the different parameters studied above, we introduce a simple solution based on the working assumption that the equilibrium temperature of the system results from the average value of the ligand fields. To express analytically the equilibrium temperature, we consider only the nearest neighbors in our development. In a core-shell structure, the interactions between

molecules are not the same depending on their positions. The nodes in the core part experience the same kind of interaction with their four nearest neighbors, unlike those located at the interface core/shell. For the latter case, we assume that nodes located at the interface have two nearest neighbors on the core and two nearest neighbors on the shell. In the case of a particle whose R is the radius and a the thickness of the shell, we count $\pi(R - a)(R - a - 2)$ nodes in the core part and $2\pi(R - a)\omega$ nodes on the core/shell interface, where ω is a unit distance required for dimensional homogeneity. Such analysis leads to the following expression of the equilibrium temperature derived from Eq. (8) by setting $h_i = 0$:

$$T_{eq} = \frac{\Delta}{k_B \ln g} + \frac{4A_0 \rho_1}{k_B \ln g}\left[\frac{-\rho_1 \omega}{(R-a)} - 2(\langle r \rangle_{T_{eq}} - \rho_0)\right]. \quad (9)$$

To assess the enriching contribution of the above electroelastic model and to suggest possible explanations for the experimental results related to spin crossover nanoparticles in a core-shell structure, it is necessary to understand how the thermal hysteresis loop connects to the different structural parameters. For that, let us make a detailed investigation of the equilibrium temperature and hysteresis width as a function of various parameters, such as the particle size, the interaction strength, the shell's stiffness, and the shell's thickness. The average properties of the system are represented by means of the HS fraction, n_{HS}, defined as

$$n_{HS} = \frac{(1 + \langle S_i \rangle)}{2}, \quad (10)$$

which represents the probability of occupying the HS state at a given temperature. The transition temperature (called also the equilibrium temperature), T_{eq}, and the hysteresis width ΔT are estimated numerically as

$$T_{eq} = \frac{T^{HS \to LS} + T^{LS \to HS}}{2}, \quad \Delta T = T^{HS \to LS} - T^{LS \to HS}, \quad (11)$$

where $T^{HS \to LS}$ and $T^{LS \to HS}$ are the transition temperature in the cooling and warming processes, respectively.

A. Dependence on the particle size

To analyze the effect of nanoparticle size, we have considered πR^2 molecules (where R is the radius of the particle comprised in the range 4–20 nm) interacting elastically with an elastic constant $A_0 = 10^5$ K/nm^2. The thickness of the shell was fixed to 2 nm. The obtained results are reported in Fig. 2 and they undeniably exhibit a size dependence of the thermal variation of the HS fraction. Thus, the reduction of the particle size induces a shift of the hysteresis to lower temperature as well as a narrowing of the hysteresis aperture, in good agreement with the experimental observations [15,17,31]. However, and surprisingly, the cooperative behavior of the transition appears to be less sensitive to the size modification, since the system maintains the first-order character even at small particle sizes. According to Eq. (9), the equilibrium temperature has a rational behavior as a function of the particle radius in particular when $R \gg a$. The fit (red line) of the simulated results of the equilibrium temperature (open circles) using the approximated theoretical expression (9) indicates that for a large system the equilibrium temperature
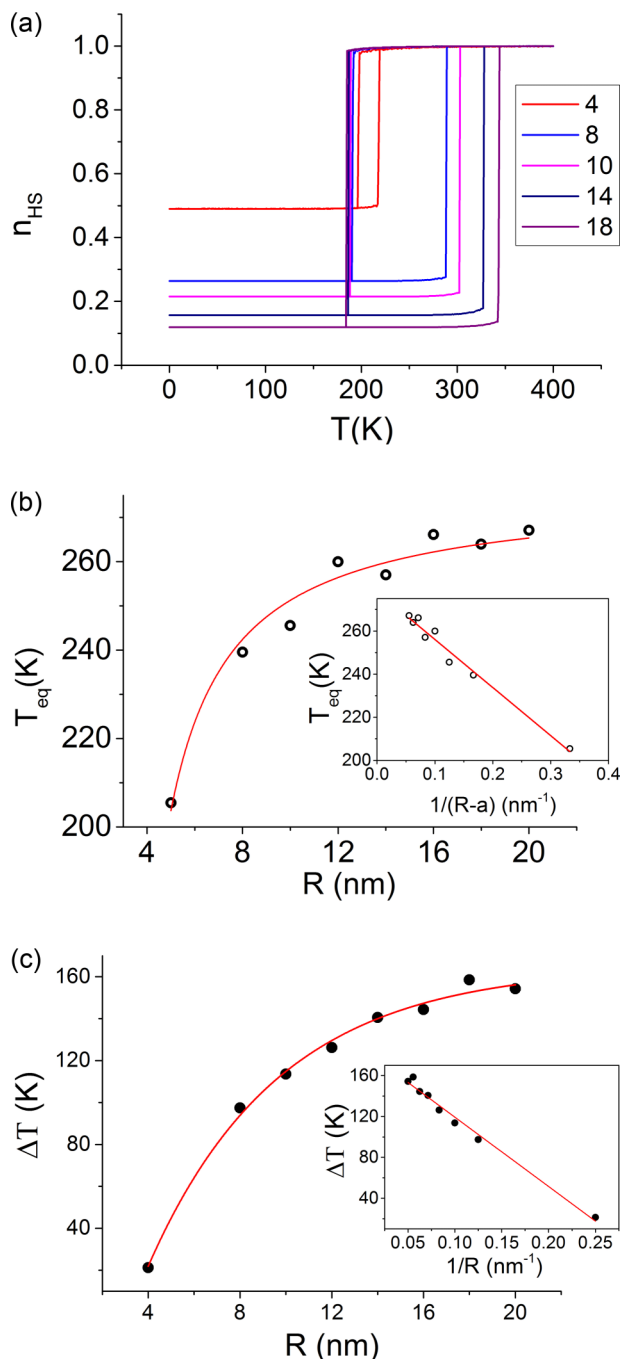
FIG. 2. (Color online) (a) Thermal hysteresis for different particle sizes. (b) Transition temperature vs the particle's radius, R. Inset: transition temperature vs $1/(R - a)$, showing a linear plot. (c) The hysteresis loop width (ΔT) vs R, and in the inset, ΔT vs of $1/R$, showing a linear plot. The figures were computed using the parameter values $A_0 = 10^5$ K/nm^2 and $a = 2$ nm.

hysteresis width of a macroscopic system ($R \rightarrow \infty$), and we find here $T_{eq}^{R \rightarrow \infty} \approx 278$ K and $\Delta T^{R \rightarrow \infty} \approx 184$ K, respectively. $T_{eq}^{R \rightarrow \infty}$ could also be evaluated from Eq. (9) as

$$T_{eq}^{R \rightarrow \infty} = \frac{\Delta}{k_B \ln g} + \frac{4 A_0 \rho_1}{k_B \ln g}[-2(\langle r \rangle_{T_{eq}} - \rho_0)] \approx 272 \text{ K},$$

$$(12)$$

a value that agrees quite well with that of the simulation. To well understand the origin of the small deviation (2%) between the simulation and the analytical prediction, we should mention that for a free boundary problem (a spin crossover system without forced HS atoms on the surface), the term $(\langle r \rangle_{T_{eq}} - \rho_0)$ in Eq. (9) must strictly vanish at the transition temperature due to the equiproportionality of the HS and LS fractions, where $\langle r \rangle = \rho_0 = R_0^{HL}$. However, in the present case the situation is different, especially from the structural point of view, due to the presence of forced HS atoms on the surface. Indeed, the shell, whose lattice parameter is that of the HS state (i.e., quite large), applies a "negative" stress on the core part of the particle and tends to increase the lattice parameter of the equilibrium structure, which always remains larger than ρ_0 at equilibrium (i.e., when we have equipopulation between the HS and the LS of the core). Therefore, this effect was not accounted for in the analytical expression (12).

Although the decreasing trend of the equilibrium temperature as a function of the system's size has already been reported in the case of square-shaped nanoparticles [26], it should be noticed that the rational law of T_{eq} as a function of the size, found in the present work, deviates from that estimated in [26], in which T_{eq} behaves as $T_{eq} \propto \sqrt{\ln (L - L_0)}$, where L denotes the size of the nanoparticle and L_0 is the smallest size from which the system can convert from LS to HS. This difference between the two studies is attributed to the difference in the lattice's shape (circular and square), thus indicating the importance of this parameter. Additionally, one can easily remark that the transition temperatures $T^{HS \rightarrow LS}$ and $T^{LS \rightarrow HS}$ do not behave similarly [see Fig. 2(a)]. Actually, while $T^{HS \rightarrow LS}$ remains insensitive to the particle size change, $T^{LS \rightarrow HS}$ clearly increases with the radius R. This demonstrates that the LS state is stabilized when we increase the particle radius, R, and then the negative stress applied by the shell has less of an effect on the core part. This feature can be understood by considering that the effect of the shell is weighted by the ratio shell/core: $\frac{R^2 - (R-a)^2}{(R-a)^2} \simeq 2\frac{a}{R}$, which straightforwardly vanishes when $R \gg a$.

B. Effect of the stiffness of the shell

Here, we use a radius value $R = 12$ nm and a shell thickness $a = 3$ nm, which are maintained constant in the simulations. Our first goal was to check how the elastic constant, A_0, acts on the thermal spin transition based on the assumption that the shell and the core have the same elastic constant, A_0. The corresponding results are summarized in Fig. 3. As expected, by changing the value of A_0, the nature of the transition could be changed. Indeed, as the interaction becomes weak, the transition moves from first order to gradual (Boltzmann distribution). Furthermore, Figs. 3(a) and 3(b) reveal that when the value of A_0 is decreased, the thermal hysteresis loop

becomes rather constant, which corresponds to the bulky behavior. Furthermore, the equilibrium temperature as well as the hysteresis width behave linearly as a function of the inverse of the particle radius, as illustrated in the insets of Figs. 2(b) and 2(c). At this stage, we should mention that the intercepts derived from the linear fit of T_{eq} and that of ΔT as a function of $1/R$ correspond to the equilibrium temperature and
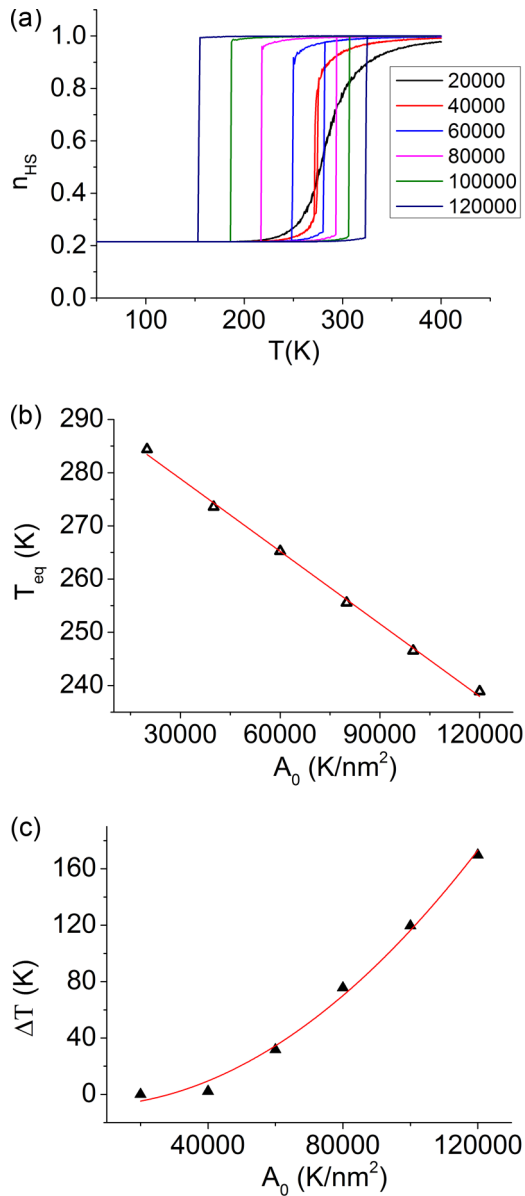
FIG. 3. (Color online) (a) Thermal hysteresis for different interactions between molecules. (b) Evolution of the equilibrium temperature as a function of the elastic constant A_0. (c) Width of the hysteresis as a function of the elastic constant A_0. (Computed for $R = 12$ nm and $a = 3$ nm.)

shifts to a lower temperature [see Fig. 3(b)] with a narrowing of the hysteresis aperture [see Fig. 3(c)]. This fact agrees with the previous tendencies reported in the different elastic models based on a deformable lattice [25,27,32–36]. The linear behavior of the equilibrium temperature as a function of the elastic constant, A_0, is remarkable in Eq. (9). Such behavior is a consequence of the contribution of the elastic field, $-A_0 \rho_1 \sum_{j=1}^{z} (r_{ij} - \rho_0)$ [see Eq. (8)], to the total ligand field energy, and this term is one of the most important contributions of the interactions between the electronic and the elastic degrees of freedom in this problem. In the case of a system without a shell, the latter term should be negative in the HS state and positive in the LS state. This reasoning is quite

general and remains valid as soon as we consider that the shell has the same elastic properties (i.e., stiffness and equilibrium distances) as those of the HS state. One can wonder whether the slope of the $T_{eq}(A_0)$, depicted in Fig. 3(b), becomes positive. For that, the condition $\frac{-\rho_1 \omega}{(R-a)} > 2(\langle r \rangle_{T_{eq}} - \rho_0)$ [derived from Eq. (9)] should be satisfied. This is impossible, since $\langle r \rangle_{T_{eq}}$ is always bigger than ρ_0 due to the existence of a forced HS molecules on the surface. The latter contributes to the negative slope of T_{eq} and promotes the HS state, explaining the asymmetric shift of the transition temperature $T^{HS \to LS}$ and $T^{LS \to HS}$ of the hysteresis loops.

Turning to the effect of shell stiffness, now we study the general case in which the shell and the core of the particle do not have the same elastic constants. Hereafter, we keep unchanged the elastic constant of the core part as $A_0 = 10^5$ K nm^{-2} and we tune the elastic constant Z of the shell in the range 10^4–10^6 K nm^{-2}. It is important to mention that for the sake of simplicity, the equilibrium distances between the neighboring atoms in the shell have been set equal to those of the HS state, and they are also kept unchanged when we vary Z. The corresponding results are summarized in Figs. 4(a)–4(c), which reveal that a soft shell ($Z \ll A_0$) leads to a narrow hysteresis (in contrast to rigid shells, which induce a large hysteresis width). Moreover, Fig. 4(a) shows that the transition temperature upon cooling (HS $\to$ LS) is less sensitive to the rise of the shell's stiffness, unlike that of (LS $\to$ HS), which remarkably increases with Z. To understand these results, one has to consider that the first-order transition studied here is accompanied by the volume change of the core part, and so any pressure effect on the core will delay the transition. This is what happened when we increased the rigidity of the shell, which then hinders the volume change of the core. For higher (lower) Z values, a higher (lower) equilibrium temperature results, as depicted in Fig. 4(b). However, the evolution of the associated thermal hysteresis width shows also an increasing behavior with Z. Such a fact is clearly different from the usual pressure effect in SC solids that is accompanied by the vanishing of the first-order character of the transition at high-pressure values. Consequently, the present situation is much more subtle since the variation of the stiffness also affects the cooperativity of the core part. Increasing Z results in an increase of the effective elastic interaction of the system, which leads to an increase of the hysteresis width. It is worth mentioning that this behavior is not trivial and cannot be explained by the usual Ising-like models, which do not account for the elastic effects. Furthermore, Fig. 4(b) shows a nonlinear dependence of the thermal transition regarding the shell stiffness. Indeed, one can notice the presence of a threshold value $Z^{th} \simeq A_0 = 10^5$ K/nm^2 above which the equilibrium temperature converges to the limit $T_{eq} = 190$ K. A similar behavior is also observed for the thermal hysteresis width. These results indicate that beyond the elastic constant A_0 of the SCO core, a further increase in the shell's stiffness does not influence significantly the core part. It is worth mentioning that the present case simulates quite well a spin crossover particle (core part) embedded in a matrix (shell) having different elastic properties. In Ref. [22], the authors investigated the magnetic behavior of Fe(pyrazine)Pt(CN)$_4$ spin crossover nanoparticles within a different matrix, and they found that a lower cooperative transition was observed in the case
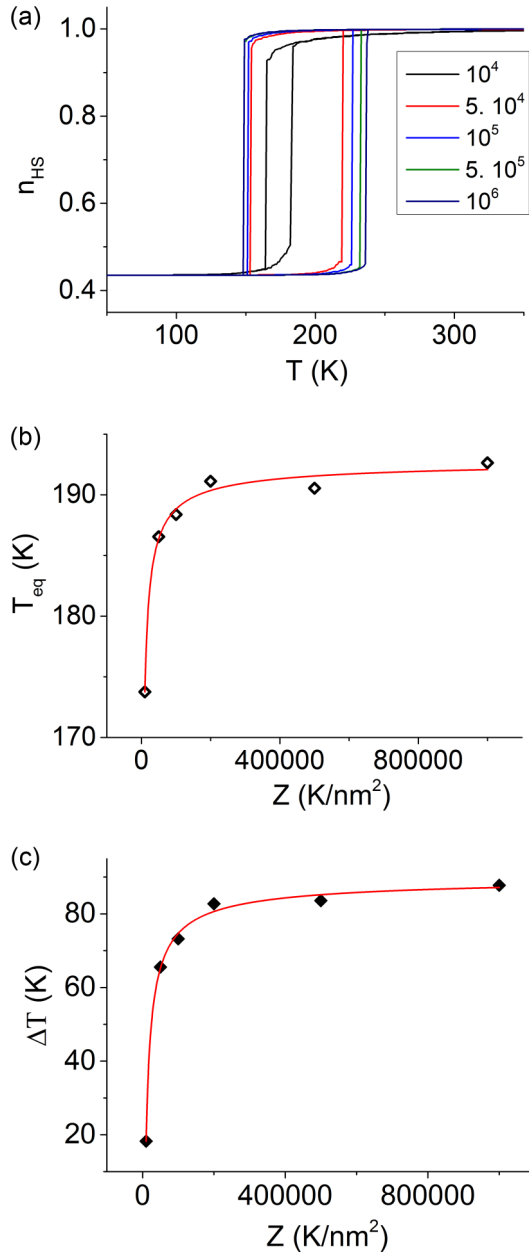
FIG. 4. (Color online) (a) Thermal hysteresis for different values of the shell rigidity, Z. Evolution of the equilibrium temperature (b) and the hysteresis width (c) as a function of Z. (Computed for $R = 12$ nm, $a = 3$ nm, and $A_0 = 10^5$ K/nm^2.)
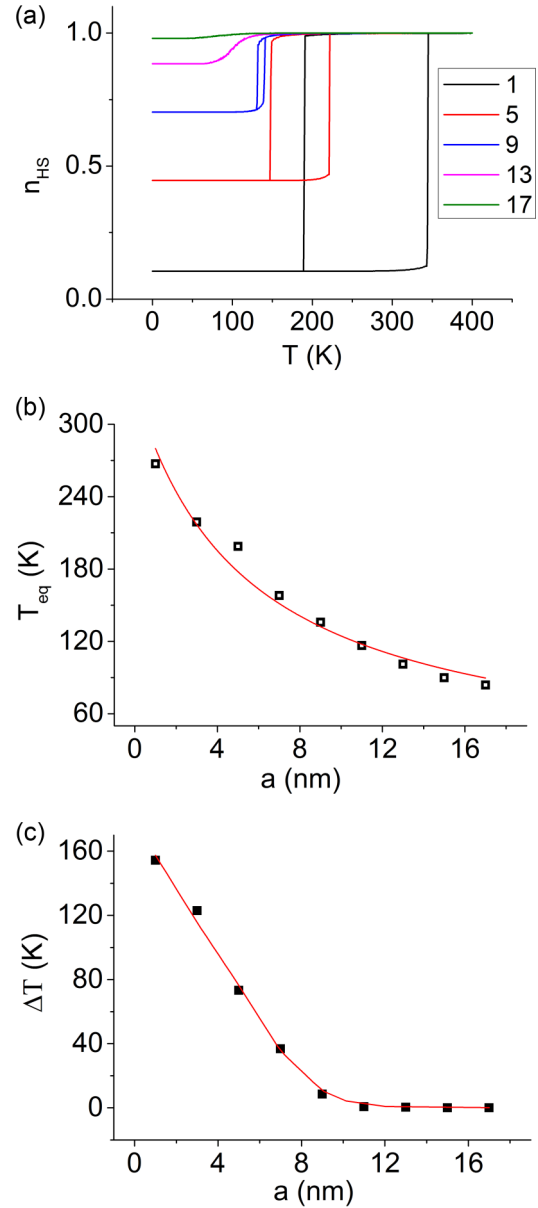

FIG. 5. (Color online) (a) Thermal hysteresis as a function of the thickness of the shell. (b) Evolution of the equilibrium temperature as a function of the thickness of the shell a. (c) Width of the thermal hysteresis loop as a function of the thickness of the shell. (Computed for $A_0 = Z = 10^5$ K/nm^2 and $R = 20$ nm.)

of a compressible matrix, which is consistent with our simulations.

C. Dependence on the thickness of the shell

To study the shell's thickness effect, we have considered a lattice with a radius $R = 20$ nm and we have fixed the elastic constant of the whole system (core and shell) to $A_0 = Z = 10^5$ K nm^{-2}. The equilibrium distance of the shell was taken independent of its size and equal to that of the HS phase. The analysis was performed by varying the value of a from 2 to 17 nm and keeping the core's radius, R, as constant. The thermal dependence of the HS fraction, given in Fig. 5(a),

shows that the thickness of the shell acts simultaneously on the transition temperature and the hysteresis width [see Figs. 5(b) and 5(c)]. In fact, as the thickness of the shell increases, the transition temperature shifts downward and the hysteresis vanishes. In a first attempt, this behavior may seem surprising, since usually when the transition temperature decreases, the hysteresis width increases. However, one can remark that this behavior resembles that of Fig. 2, showing the variation of the thermal hysteresis of the nanoparticle as a function of the core's size, and it can be described by a rational law as expressed in Eq. (9). Indeed, when the shell is very thick (see the case in which $a = 17$ nm in Fig. 5), the average atomic distances, $\langle r \rangle$, increase and may reach the limiting value $\langle r \rangle \simeq R_0^{HH}$,

obtained for an infinite shell. According to Eq. (9), this effect will lower the equilibrium transition by the quantity

$$\Delta T_{\text{eq}} = \frac{4 A_0 \rho_1}{k_B \ln g} \left(\frac{-\rho_1 \omega}{(R-a)} - 2(\langle r \rangle_{T_{\text{eq}}} - \rho_0) \right), \qquad (13)$$

in good agreement with the results of the numerical simulations reported in Fig. 5(b). This lowering of the transition temperature is accompanied by a decrease of the hysteresis loop, i.e., of the strength of the elastic interactions responsible for the spin transition in the system. The hysteresis vanishes as a result of a weak ratio between the surface of the electroelastically active core and that of the electronically inert (but elastically active) shell. So, a thicker shell induces naturally an important residual HS fraction due the expanded lattice and consequently hinders the elastic interactions between the spin crossover units by reducing all the internal pressures and the elastic stresses that drive the first-order transition. Indeed, in such a situation, the LS state is no longer rigid and it resembles the HS state, therefore the internal elastic forces responsible for the cooperative nature of the transition vanish, which leads to the gradual spin crossover transitions obtained in Fig. 5(a). This is particularly true for $a > 11$ nm as revealed in Fig. 5(c), a value that can be assigned as the threshold shell thickness above which the thermal hysteresis loop disappears. These results agree well with the experimental observations [22], where the authors observed the presence of a large hysteresis for nanoparticles of Fe(pyrazine)Pt(CN)$_4$ coated with a thin silica shell while a very small aperture was observed for a diluted system, which corresponds to a thick shell.

IV. CONCLUSION

We investigated the thermal spin transition of nanoparticles in a core-shell structure, where the shell is simulated by forced HS molecules on the surface, by means of an electroelastic model. The thermal spin transition was monitored as a function of the size of the particle, the intensity of the interactions between the molecules, as well as the stiffness of the shell and its thickness. Such analysis clearly reveals dependent behaviors as a function of the latter parameters and highlights the crucial influence of the core-shell structure on the thermal transition. Our main conclusions include the following: (i) a reduction of the size of the particle induces a shift of the hysteresis loop to a lower temperature with a narrowing of the hysteresis loop, (ii) the shell could contribute significantly in the shift of the hysteresis loop toward lower temperatures by applying a negative stress on the active SCO core of the particle, and (iii) the presence of a large hysteresis with a first-order transition is coupled with a thin and stiff shell. Such behaviors underline the crucial role of the surrounding environment of the spin crossover core part of the particle. Our findings not only agree well with the experimental observations but also provide potential explanations, based on elastic consideration, of some behaviors of the thermal spin transition. Furthermore, our study highlights the crucial impact of the system shape on the behavior law describing the variation of the equilibrium temperature as a function of the size of the particle, where a dramatic change was observed between the circularly shaped and the square-shaped lattices. It is interesting to mention that the reasoning developed here (based on the elasticity) that describes the interaction of the spin crossover part with its immediate surrounding environment is not limited to the core-shell structure only, but could be extended to the case of spin crossover nanoparticles embedded in some matrix.

[1] *Topics in Current Chemistry, Spin Crossover in Transition Metal Compounds I-III*, edited by P. Gütlich and H. A. Goodwin (Springer, Heidelberg, 2004), pp. 233–235.

[2] P. Gütlich, Struct. Bonding (Berlin) **44**, 83 (1981).

[3] P. Gütlich, A. Hauser, and H. Spiering, Angew. Chem. Int. Ed. Engl. **33**, 2024 (1994).

[4] E. König, Struct. Bonding (Berlin) **76**, 51 (1991).

[5] O. Kahn and C. J. Martinez, Science **279**, 44 (1998).

[6] A. Bousseksou, K. Boukheddaden, M. Goiran, C. Consejo, M-L. Boillot, and J-P. Tuchagues, Phys. Rev. B **65**, 172412 (2002).

[7] W. Kosaka, K. Nomura, K. Hashimoto, and S. Ohkoshi, J. Am. Chem. Soc. **127**, 8590 (2005).

[8] D. Papanikolaou, W. Kosaka, S. Margadonna, H. Kagi, S. Ohkoshi, and K. Prassides, J. Phys. Chem. C **111**, 8086 (2007).

[9] F. Prins, M. Monrabal-Capilla, E. A. Osorio, E. Coronado, and H. S. J. van der Zant, Adv. Mater. **23**, 1545 (2011).

[10] A. Bousseksou, F. Varret, M. Goiran, K. Boukheddaden, and J.-P. Tuchaguess, Top. Curr. Chem. **235**, 65 (2004).

[11] E. Coronado, J. R. Galán-Mascarós, M. Monrabal-Capilla, J. García-Martínez, and P. Pardo-Ibáñez, Adv. Mater. **19**, 1359 (2007).

[12] J. R. Galán-Mascarós, E. Coronado, A. Forment-Aliaga, M. Monrabal-Capilla, E. Pinilla-Cienfuegos, and M. Ceolin, Inorg. Chem. **49**, 5706 (2010).

[13] A. Rotaru, F. Varret, A. Gindulescu, J. Linares, A. Stancu, J. F. Létard, T. Forestier, and C. Etrillard, Eur. Phys. J. B **84**, 439 (2011).

[14] T. Forestier, S. Mornet, N. Daro, T. Nishihara, S. Mouri, K. Tanaka, O. Fouche, E. Freysz, and J.-F. Létard, Chem. Commun. **36**, 4327 (2008).

[15] T. Forestier, A. Kaiba, S. Pechev, D. Denux, P. Guionneau, C. Etrillard, N. Daro, E. Freysz, and J.-F. Létard, Chem. Eur. J. **15**, 6122 (2009).

[16] L. Salmon, G. Molnar, D. Zitouni, C. Quintero, C. Bergaud, J.-C. Micheau, and A. Bousseksou, J. Mater. Chem. **20**, 5499 (2010).

[17] I. Boldog, A. B. Gaspar, V. Martinez, P. Pardo-Ibanez, V. Ksenofontov, A. Bhattacharjee, P. Gütlich, and J. A. Real, Angew. Chem., Int. Ed. **47**, 6433 (2008).

[18] C. Bartual-Murgui, N. A. Ortega-Villar, H. J. Shepherd, M. C. Munoz, L. Salmon, G. Molnar, A. Bousseksou, and J.-A. Real, J. Mater. Chem. **21**, 7217 (2011).

[19] J. Larionova, L. Salmon, Y. Guari, A. Tokarev, K. Molvinger, G. Molnar, and A. Bousseksou, Angew. Chem., Int. Ed. **47**, 8236 (2008).

[20] A. Tissot, C. Enachescu, and M.-L. Boillot, J. Mater. Chem. **22**, 20451 (2012).

[21] F. Volatron, L. Catala, E. Rivière, A. Gloter, O. Stéphan, and T. Mallah, Inorg. Chem. **47**, 6584 (2008).

[22] Y. Raza, F. Volatron, S. Moldovan, O. Ersen, V. Huc, C. Martini, F. Brisset, A. Gloter, O. Stéphan, A. Bousseksou, L. Catala, and T. Mallah, Chem. Commun. **47**, 11501 (2011).

[23] A. Muraoka, K. Boukheddaden, J. Linares, and F. Varret, Phys. Rev. B **84**, 054119 (2011).

[24] L. Stoleriu, P. Chakraborty, A. Hauser, A. Stancu, and C. Enachescu, Phys. Rev. B **84**, 134102 (2011).

[25] S. Titos-Padilla, J. M. Herrera, X.-W. Chen, J. J. Delgado, and E. Colacio, Angew. Chem., Int. Ed. **50**, 3290 (2011).

[26] H. Oubouchou, A. Slimani, and K. Boukheddaden, Phys. Rev. B **87**, 104104 (2013).

[27] A. Slimani, K. Boukheddaden, F. Varret, H. Oubouchou, M. Nishino, and S. Miyashita, Phys. Rev. B **87**, 014111 (2013).

[28] K. Boukheddaden, I. Shteto, B. Hoo, and F. Varret, Phys. Rev. B **62**, 14796 (2000).

[29] W. C. Yu and P. Gielisse, Mater. Res. Bull. **6**, 621 (1971).

[30] A. Bousseksou, J. Nasser, J. Linares, K. Boukheddaden, and F. Varret, J. Phys. **2**, 1403 (1992).

[31] V. Martinez, I. Boldog, A. B. Gaspar, V. Ksenofontov, A. Bhattacharjee, P. Gütlich, and J. A. Real, Chem. Mater. **22**, 4271 (2010).

[32] S. Miyashita, Y. Konishi, M. Nishino, H. Tokoro, and P. A. Rikvold, Phys. Rev. B **77**, 014105 (2008).

[33] M. Nishino, K. Boukheddaden, Y. Konishi, and S. Miyashita, Phys. Rev. Lett. **98**, 247203 (2007).

[34] M. Nishino, C. Enachescu, S. Miyashita, K. Boukheddaden, and F. Varret, Phys. Rev. B **82**, 020409(R) (2010).

[35] C. Enachescu, L. Stoleriu, A. Stancu, and A. Hauser, Phys. Rev. Lett. **102**, 257204 (2009).

[36] W. Nicolazzi and S. Pillet, Phys. Rev. B **85**, 094101 (2012).